https://doi.org/10.20965/ijat.2017.p0869

Paper:

Fundamental Study on Addition of Osteoconductivity to Titanium Alloy Surface by EDM

Togo Shinonaga†, Yuta Iida, Ryota Toshimitsu, and Akira Okada

Graduate School of Natural Science and Technology, Okayama University
3-1-1 Tsushima-naka, Kita-ku, Okayama 700-8530, Japan
†Corresponding author, E-mail: shinonaga@okayama-u.ac.jp
[Received January 17, 2017; accepted April 18, 2017]

In recent years, one common cure for losses in joint function caused by osteoarthritis or rheumatoid arthritis is replacement with an artificial joint. For this reason, it is necessary to add osteoconductivity to artificial joint component surfaces that make contact with bone, thereby reducing the period of time necessary to fixate the bone tissue and the artificial joint component. With the intent of efficiently machining the joint shape by electrical discharge machining (EDM) and simultaneously formation of a surface with osteoconductivity, this study discusses the possibility of adding osteoconductivity to a titanium EDMed surface.

Keywords: electrical discharge machining (EDM), osteoconductivity, artificial joint component

1. Introduction

In recent years, a common cure for losses in joint function caused by osteoarthritis or rheumatoid arthritis is replacement with an artificial joint [1, 2]. Currently, two main procedure types are in clinical use to fixate an artificial joint component to a bone. One uses bone cement, while the other (cementless) does not. In the cement fixation procedure, an artificial joint component and bone are adhered with bone cement, which contains poly methyl methacrylate as a main component. The procedure requires a short period of time before fixation is achieved. However, cement deterioration reduces the cementing strength over time. In addition, reports have been made of the necrosis of bone tissue caused by excessive compression and fever at the time the bone cement is filled [3], as well as of reductions in blood pressure and shock symptoms caused by the cement monomer components [4]. For this reason, cementless fixation procedures are typically used in current clinical practice. Examples of cementless fixation procedures include a method by which a porous material is provided on the artificial joint surface and fixated in the pore by the anchor effect associated with a new bone intrusion. This method has high biocompatibility and safety because it does not use bone cement. However, a long period of time is necessary before fixation occurs, lasting several months before complete fixation of bone tissue to the artificial joint is achieved [3]. For this reason, social rehabilitation may be significantly delayed because of the muscle weakness caused by long hospital stays.

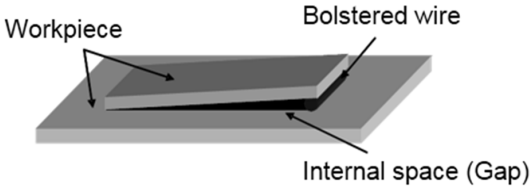

Fig. 1. Generation of gap between two titanium plates [13].

Materials which have high biocompatibility with bone, such as hydroxyapatite, can be coated on the bone junction surface of an artificial joint component to add osteoconductivity [5], which is the ability to facilitate the growth of the new bone using the coated material as a scaffold, to the artificial joint component material surface. As a currently practiced method, osteoconductive hydroxyapatite can be directly coated onto the bone junction of the artificial joint using plasma spraying [6–9]. However, a clear interface exists between the base material and the coating layer, so the delamination of the coating layer is seen as a problem. In addition, the hydroxyapatite is exposed to high temperatures during plasma spraying; hence, its composition and crystalline properties cannot be maintained and its composition changes.

Meanwhile, a rutile titanium oxide (TiO_2) layer can be obtained by providing an oxidation treatment to the surface of titanium-series materials [10–12]. This surface layer can spontaneously deposit apatite in body fluid [11, 12]. Methods to form a titanium oxide layer on a titanium-series metal surface include thermal treatment. Even for thermally oxidized metal titanium immersed in simulated body fluid (SBF) for long periods, hydroxyapatite does not spontaneously deposit. However, as presented in **Fig. 1**, Sugino et al. [13] reported that, when two heat-treated titanium plates were placed with a certain gap distance, hydroxyapatite deposited on the internal surfaces. In other words, by machining a surface shape with the appropriate gap space and adding a thermal oxidation treatment, it is possible to add the ability of spontaneous bone-like apatite formation in a body-fluid environment to an artificial joint, and this can develop into

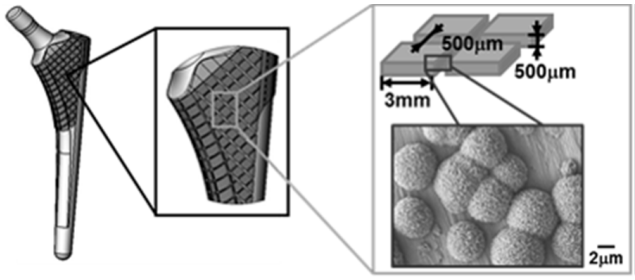

Fig. 2. Stem design for high osteoconductivity [13].

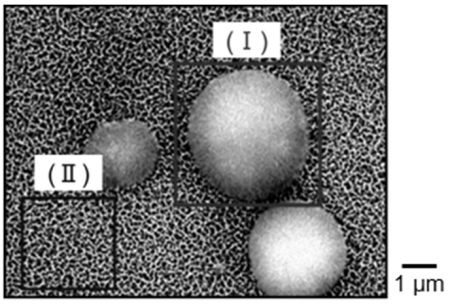

(a) SEM image of CHT sample after soaking in SBF.

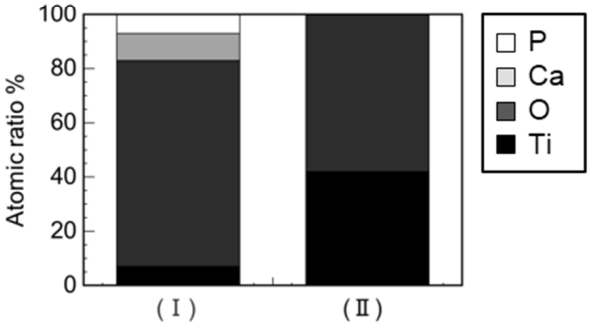

(b) Component analysis of CHT sample after soaking in SBF.

Fig. 3. SEM image and component analysis of CHT sample after soaking in SBF.

osteoconductivity. In addition, it is known that a designed groove shape, as an example of an appropriate gap space, of 0.8 mm or smaller in width shows significantly developed bone-like apatite formation ability [13].

As presented in **Fig. 2**, one method currently under development for practical use exists in which osteoconductivity is added to an artificial hip joint stem surface by providing thermal oxidation treatment after a finely grooved pattern of an appropriate scale is machined on the surface. However, the required groove shape has a fineness of submillimeter order, and the excellent mechanical characteristics of titanium-series metals cause difficulties in machining of the grooves by cutting workpiece in terms of the machining efficiency and tool cost. The thermal oxidation treatment also requires some hours. Therefore, efficiency improvements are strongly demanded. In contrast to these methods, Mizutani et al. [14, 15] reported that a microstructures and a titanium oxide layer could be simultaneously formed on pure titanium by irradiating with nanosecond pulsed laser.

This study proposes the machining of a fine groove shape on a titanium-series metal surface by electrical discharge machining (EDM) [16, 17], which is a thermal processing method unaffected by the mechanical characteristics of a workpiece and easily capable of fine shape machining. The machining surface is simultaneously oxidized by using deionized water as the machining fluid. This is intended to form an osteoconductive surface structure in a very efficient manner, with which fine groove machining of the titanium series metal surface and the formation of a thermally oxide layer are achieved simultaneously. The surface texture of a titanium alloy machined surface produced by EDM was analyzed and basic examination on a possibility of addition of osteoconductivity was carried out.

2. Experimental Method

2.1. Osteoconductivity Evaluation Method

For the purpose of the basic evaluation of the hydroxyapatite formation ability of an EDMed surface, a flat EDMed surface was selected as the target in this study, instead of a groove shape. An EDMed titanium-series material surface was immersed for seven days in 30 mL of 36.5°C SBF with the surface facing downwards and with appropriate gap spaces provided between the surface and a polytetrafluoroethylene. The apatite formation ability of the EDMed surface was evaluated. This evaluation method using SBF is effective as a method for evaluating biocompatibility in vitro [18, 19] and is registered by the International Standard Organization (ISO) [20]. Adopting an evaluation using SBF, this study examined the possibility of the addition of osteoconductivity by EDM based on the deposition of hydroxyapatite or its equivalent calcium phosphate series on the machined surface.

In order to check the performance of the created SBF, an evaluation of CHT (chemical treatment with H_2O_2 solution and subsequent heat treatment) sample was firstly performed. Pure titanium was left in 80°C H_2O_2 solution with the mass concentration of 3% for 180 minutes and then left in 400°C atmosphere for 60 minutes, so that a titanium oxide layer was formed on the substrate surface. This CHT sample surface had a very high bone formation ability, and the performance of SBF was confirmed by using it. **Fig. 3** presents a scanning electron microscopy (SEM) image of the CHT sample surface after immersion in SBF and a component analysis result from energy-dispersive X-ray spectroscopy (EDX). In general, the initial precipitation shape of hydroxyapatite is semispherical. The semispherical portion observed using SEM matches this characteristic geometry of hydroxyapatite. In addition, the component analysis results from the semispherical portion (I) and the non-semispherical portion (II) of the surface indicate the detection of Ca and P from the semispherical portion (I), which clearly indicates hydroxyapatite formation. This demonstrates that the SBF has an appropriate performance for evaluating osteoconductivity.

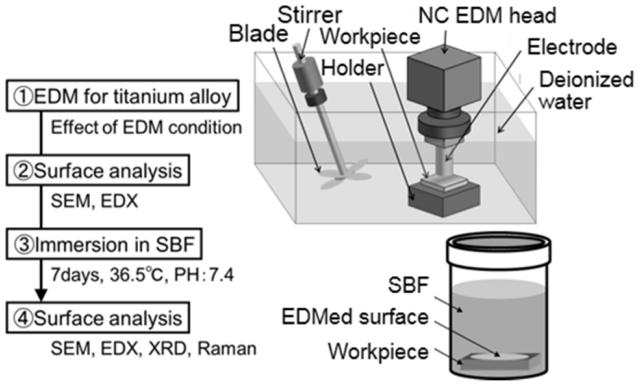

Fig. 4. Experimental chart.

Table 1. Discharge conditions for die sinking EDM with copper electrode.

Conditions	Discharge current i_e (A)	Pulse duration t_e (μs)	Pulse interval time t_o (μs)	Electrode polarity
I-1	3	50	100	-
I-2	9	25	50	-
I-3	9	50	100	-
I-4	9	100	200	-
I-5	15	50	100	-
I-6	9	50	100	+

2.2. Experimental Procedure

The procedure of this study is presented in **Fig. 4**. First, a machining surface is formed by using deionized water as the machining fluid, copper as the electrode material in die-sinking EDM of Section 3.1, brass as the electrode material in wire EDM of Section 3.2, and brass as the electrode material in the die-sinking and wire EDM of Chapter 4 for a titanium alloy surface. Then, the component is analyzed by EDX and the machining surface is observed using SEM. Next, the specimen is immersed in SBF for seven days, and white precipitates such as hydroxyapatite are formed on the machining surface. After that, the machined surface is observed using SEM and analyzed by EDX, X-ray diffraction (XRD), and Raman spectroscopic analysis to confirm the formation of hydroxyapatite and a calcium phosphate compound.

3. Hydroxyapatite Formation Ability

3.1. Titanium Oxide Layer Formation by Die-sinking EDM

At first, formation of a rutile TiO_2 layer is examined by die-sinking EDM in deionized water. A linear motor-driven EDM apparatus (AP1L, Sodick) was used to perform machining under various conditions, such as different pulse duration and discharge currents. **Table 1** presents the machining conditions used. In this experiment, the whole workpiece surface was machined as a first step before groove machining, and we observed whether hydroxyapatite formation ability was developed on the EDMed surface. The workpiece was a titanium alloy (Ti-15Zr-4Nb-4Ta) of $10 \times 10 \times 6$ mm, and the entire surface of 10×10 mm was machined with a copper electrode. The machining time was approximately 30 minutes for each condition. The machining fluid used was deionized water with the resistivity of 700 kΩ·cm.

An optical image of the EDMed surface is presented in **Fig. 5(a)**. The figure indicates that the hue of the machined surfaces varies depending on the machining conditions. In other words, the oxidation state of the machined surface varies depending on the machining conditions. The hue is not uniform on each EDMed surface, indicating non-uniform thickness of the titanium oxide layer. In addition, thin-film XRD patterns of the machining surfaces after SBF immersion for seven days are presented in **Fig. 5(b)**. In the XRD patterns of the figure, the white rhombi represent the peaks of Ti_2O_3, the black rhombi represent the peaks of TiO, and the circles represent the peaks of Ti. As is clear from the figure, the peak of TiO and Ti_2O_3 clearly appears on all of the EDMed surfaces. However, it is indicated that the peaks of the targeted rutile phase TiO_2, do not appear; little TiO_2 exists on the EDMed surfaces. Since the titanium oxide layer seen on the EDMed surfaces has low oxygen content, the oxidization level is thought to be insufficient. Machining under conditions with larger discharge energies was also attempted, but failed to form TiO_2. In addition, effect of the electrode polarity on formation of a titanium oxide layer the EDMed surface is discussed. Comparing the XRD patterns of I-3 and I-6, many more peaks of Ti are detected from I-6. In other words, it is indicated that formation of titanium oxide layer is difficult when the electrode polarity is positive.

3.2. Titanium Oxide Layer Formation by Wire EDM

Next, formation of a rutile TiO_2 layer was tried by using a wire EDM. At first, the wire EDMed surface was evaluated by an alternating-current circuit intended to prevent an electrochemical reaction, and the formation of sufficient TiO_2 was not confirmed on the machined surfaces.

For this reason, the machined surfaces were generated by a direct-current discharge circuit that could be followed by an electrochemical reaction. In this case, the machined surface is created by the first-cut wire EDM under the conditions recommended by the machine-maker, performing the second-cut by a direct-current circuit with an offset of 0.05 mm, and performing the third-cut with no offset. By altering the average machining voltage conditions, uniform machined surfaces of different hues can be obtained. As presented in the optical microscope images of **Fig. 6**, yellow, blue, and purple colors appear in the order of ascending voltage conditions. The electrochemical reaction by the leakage current increases with increasing voltage, followed by generating uniform titanium oxide

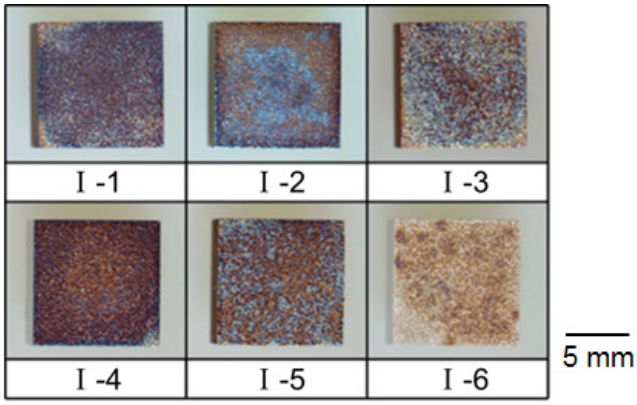

(a) EDMed surfaces with copper electrode under various machining conditions.

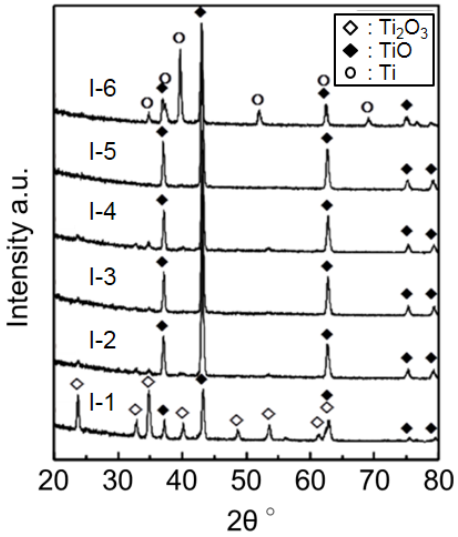

(b) XRD spectra of EDMed surfaces with copper electrode under various machining conditions.

Fig. 5. EDMed surfaces and XRD patterns with copper electrode under various machining conditions.

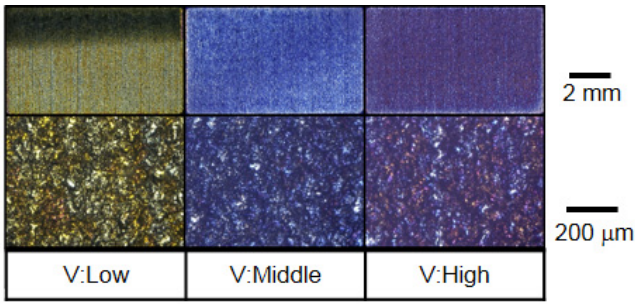

Fig. 6. Difference in wire EDMed surface with average gap voltage.

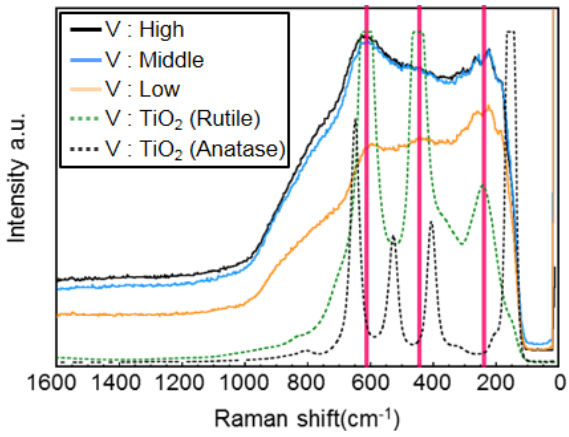

Fig. 7. Difference in Raman spectra of wire EDMed surface under various average gap voltages and TiO_2 powder.

layers of different thicknesses on the surface.

In order to confirm the formation of the TiO_2 layers, Raman spectra of the machined surfaces was obtained, as presented in **Fig. 7**. Although the EDMed surfaces are very uneven and it is therefore difficult to detect steep peaks, a few small peaks can be seen in the Raman spectra obtained from the machining surfaces. These peaks precisely match the peak positions of the Raman spectrum obtained from rutile TiO_2 powder. In other words, it is verified that rutile TiO_2 exists on the wire EDMed surfaces.

Next, these workpieces were immersed into SBF and the hydroxyapatite formation ability was evaluated. The initial precipitation shape of precipitated hydroxyapatite in SBF is semispherical, as mentioned above, and hence component analysis was provided by EDX for the spherically shaped portions on the machined surfaces. The results of SEM observation of the machined surfaces after immersion and component analysis with EDX are presented in **Fig. 8**. According to the component analysis results, Ca and P, which are components of hydroxyapatite, are not detected. Another spherically shaped portions observed at other points were also analyzed, but neither component was detected. However, since it is possible to form a rutile TiO_2 layer, which has been reported to have hydroxyapatite formation ability, it should be possible to create an osteoconductive EDMed surface if all factors obstructing hydroxyapatite formation can be successfully eliminated by widely changing the surface texture through optimizing the machining conditions.

4. Precipitation of Calcium Phosphate Compound

With the intent of precipitating hydroxyapatite on the TiO_2 layer, formation of a TiO_2 layer on the titanium alloy surface has been attempted by EDM. A white precipitate was obtained by repeating the experiment of immersing the EDMed surface in SBF. A detailed examination was performed because this white precipitate was expected to be a kind of osteoconductive calcium phosphate, similar to hydroxyapatite.

An image at the area of white precipitation is presented in **Fig. 9**. The original purpose was precipitation of hydroxyapatite. Therefore, the machined titanium was immersed such that the EDMed surface of the specimen

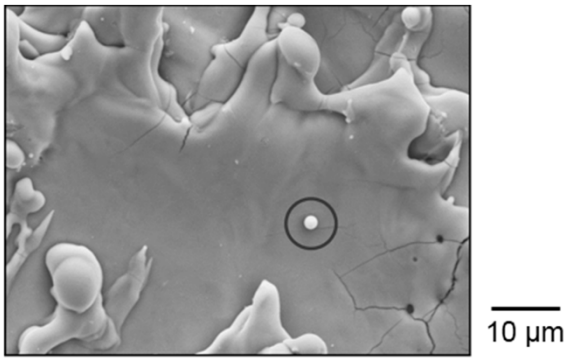

(a) SEM image of wire EDMed surface with high average gap voltage after soaking in SBF.

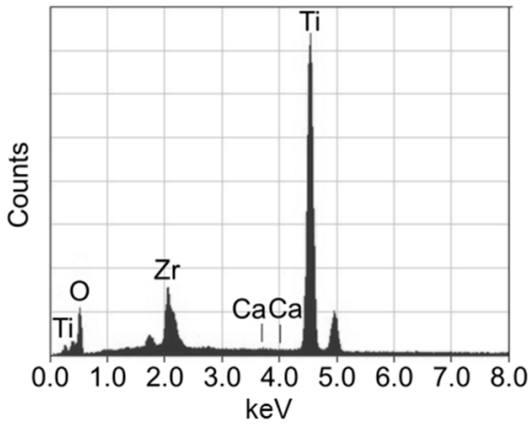

(b) EDX spectrum of wire EDMed surface with high average gap voltage after soaking in SBF.

Fig. 8. SEM image and EDX spectrum of wire EDMed surface with high average gap voltage after soaking in SBF.

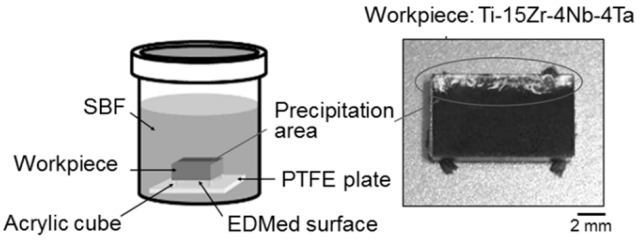

(a) Precipitation area in SBF (b) White precipitate on surface

Fig. 9. Precipitation area and image of white precipitate on surface.

faced downwards and an appropriate gap space was provided between the surface and the polytetrafluoroethylene. A great amount of white precipitation was formed in the upper area of the specimen, i.e., not on the gap space side but on the upper face side. This area is a rough machined surface by the first-cut, where wire EDM was performed with varying EDM conditions in order to cut the specimen to an appropriate size.

This rough machined surface is not uniform, but shows a slightly yellow hue at upper side of wire running (top end of the specimen). For this reason, in order to obtain a uniform machined surface, die-sinking EDM was performed in deionized water using a brass electrode. Then, under the machining conditions presented in **Table 2**, a uniform machined surface was obtained on which white material was precipitated during immersion in SBF.

Table 2. Discharge conditions for die-sinking EDM.

Electrode	Brass
Workpiece	Ti-6Al-4V
Discharge current i_e	15A
Discharge duration t_e	25 ms
Pulse interval t_0	100 ms
Working fluid	Deionized water
Electrode polarity	+

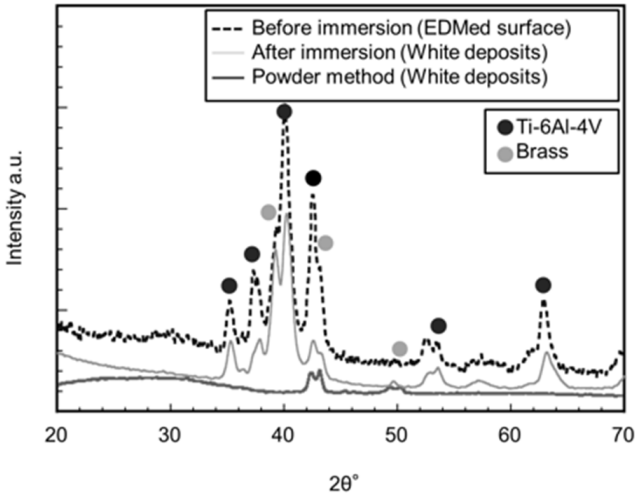

Fig. 10. XRD patterns of EDMed surface and white deposits.

4.1. Identification by XRD Analysis

An XRD analysis result of the die-sinking EDMed surface before and after immersion in SBF is presented in **Fig. 10**. The pattern before the immersion indicates peaks from the base material component and the brass electrode component used in machining. After the immersion, the peaks from the machining surface component decrease in intensity because of the precipitation of the white material. However, the peaks that presents evidence of a calcium phosphate-series component cannot be confirmed, and the white precipitate cannot be identified from the XRD pattern. Only the white material from the machining surface was collected to eliminate peaks from the base material and an analysis was performed by the powder XRD method. In this case, although the peaks of the base material component are decreased, peaks of calcium phosphate are still not confirmed. Since a clear peak from the specific material does not appear in the XRD analysis, the white precipitate is likely to have low crystallinity.

4.2. Identification by Raman Spectroscopic Analysis

Next, the white precipitate was analyzed by Raman spectroscopy, in which a microscale region of the most

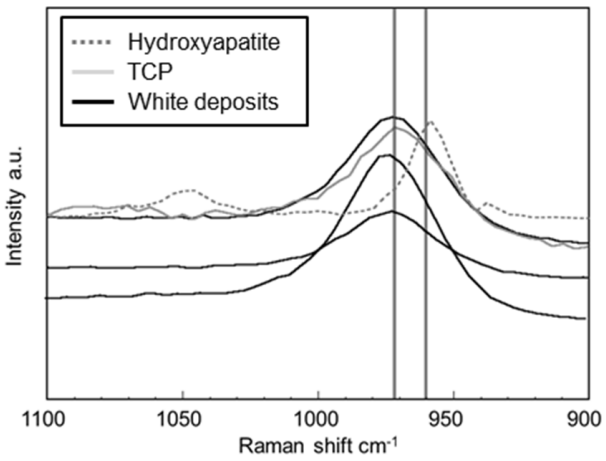

Fig. 11. Raman spectra from white deposit.

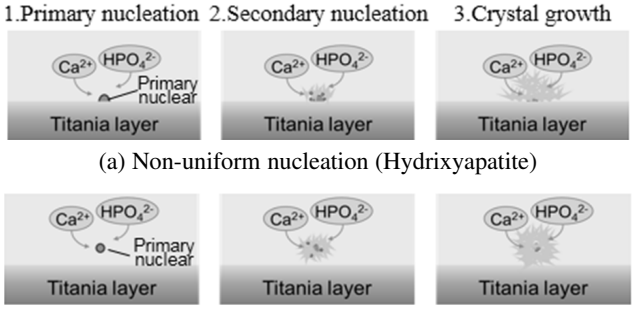

(a) Non-uniform nucleation (Hydrixyapatite)

(b) Uniform nucleation (TCP)

Fig. 12. Nucleation mechanism.

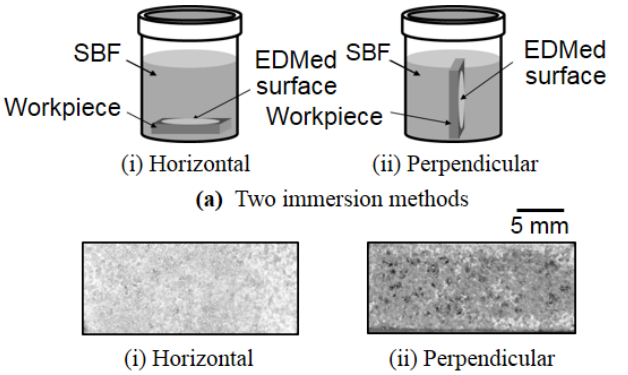

(a) Two immersion methods

(b) Optical images of EDMed surface after immersion in SBF

Fig. 13. Two immersion methods and optical images of EDMed surface.

superficial surface can be analyzed. **Fig. 11** presents the Raman spectra. The peaks obtained by analyzing the three different white materials on the machining surface are located at approximately 971 cm^{-1} each. This peak does not match the peak of hydroxyapatite, but matches the peak of tricalcium phosphate (TCP) indicated by the light solid line in the figure. This result indicates that the white precipitate is highly likely to be TCP. Similar to hydroxyapatite, TCP is a kind of osteoconductive materials. While hydroxyapatite is not well absorbed in a living body, TCP is gradually absorbed and replaced by natural bone [21].

4.3. Identification of White Material by Precipitation Mechanism

It was made clear by Raman spectroscopic analysis that the white material obtained on the die-sinking EDMed surface was highly likely to be TCP. However, the peak could differ slightly in Raman spectroscopic analysis, so the material was also identified considering its formation mechanism.

Figure 12 schematically presents the nucleation mechanism for a precipitated calcium phosphate-series material. The nucleation mechanisms of calcium phosphate-series materials are generally classified into two types; non-uniform and uniform nucleation. In non-uniform nucleation, a calcium ion and a phosphate ion in the SBF are attracted to an OH group and an oxygen ion on the specimen surface; the primary nucleus first forms on the specimen surface. Then, the calcium ion and the phosphate ion in the SBF are further bonded to the formed primary nucleus, and a crystal grows at the specimen surface. Repetition causes the particles to grow more. Meanwhile, in uniform nucleation, the primary nucleus is formed not on the specimen surface but in fluid near the surface by a specimen surface effect. After that, similar to the non-uniform nucleation, a calcium ion and a phosphate ion in the SBF are attracted and bonded to the formed primary nucleus, and a crystal grows in the fluid near the specimen. When it reaches a certain size, it makes contact with the specimen surface and is deposited. In general, hydroxyapatite precipitates via non-uniform nucleation, while TCP precipitates via uniform nucleation.

In order to confirm the precipitation mechanism of the white material, an immersion experiment was conducted with the specimen placed in the SBF so that the machined surface faced upward in the horizontal direction and sideways in the vertical direction. An outline of the immersion experiment and optical images of the specimen's machined surface after the immersion experiment are presented in **Fig. 13**. In the immersion method with the machining surface facing upwards in the horizontal direction, a sufficient amount of white material was expected to precipitate uniformly on the machining surface via either non-uniform nucleation or uniform nucleation. However, for the machined surface facing sideways in the vertical direction, a material precipitating via uniform nucleation, could not be deposited on the vertical machining surface, and hence amount of precipitate would decrease. By comparing the amount of deposited white precipitate on the machined surfaces by these immersion methods, we confirmed by which mechanism, whether non-uniform or uniform nucleation, the white material precipitated.

As demonstrated from the optical images of the specimen machined surface after the immersion experiment, the white precipitation amount is greater when the machined surface faces upwards in the horizontal direction than when the machined surface faces sideways in the vertical direction. In addition, a white floating substance is present in the fluid in which the machining surface faces

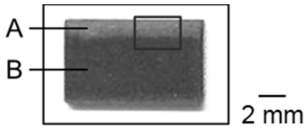

(a) EDMed surface for verification test.

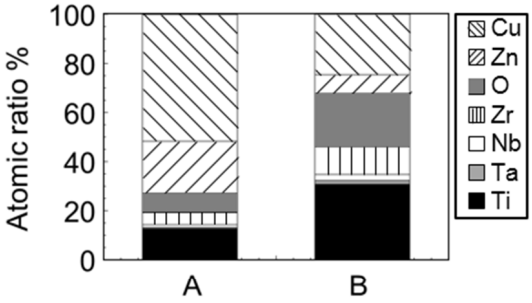

(b) Component analysis of EDMed surface.

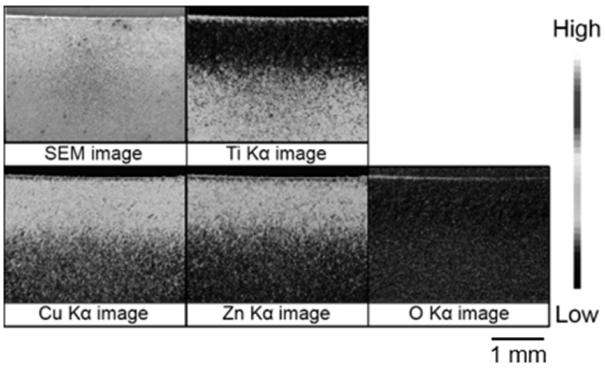

(c) SEM and Kα images of EDMed surface.

Fig. 14. EDMed surface images for verification test and component analysis.

sideways in the vertical direction. In other words, the white material precipitates via uniform nucleation, and this clearly indicates that this precipitation formed by uniform nucleation on the EDMed surface is TCP.

These results indicate that the TCP formation ability, in other words, osteoconductivity, can be added to the titanium alloy surface by EDM under the appropriate electrical conditions presented in **Table 2**.

4.4. Analysis Result of Precipitation Face by EDX

Having confirmed that the white precipitate obtained on the EDMed surface is osteoconductive TCP, the texture of the EDMed surface was examined for developing it. **Fig. 14** presents an optical image of the wire EDMed surface under the conditions for TCP to generate, component analysis results for each machined surface area by EDX, and element mapping images by Kα radiation of the different components. This machined surface was formed by EDM with the offset of 1 mm under the first-cut condition, which is the recommended condition for a steel material, and likely to be an unstable machining condition with discharge concentration. In other words, the surface is not a uniformly machined surface, and regions A and B, corresponding to a rough machined surface at upper side of wire running and a normal EDMed surface, are clearly extant. As made clear from the optical image, the hue varies within the machined surface. The variation of the hue is not from the interference of light caused by varied titanium oxide layer thicknesses. It is clearly confirmed that the material itself is adhered. As made clear from the component analysis of regions A and B seen in the optical image, while the contents of Cu and Zn are approximately 30% in total in area B of the normal EDMed surface, the Cu and Zn contents exceed 70% in area A. It is a well-known phenomenon that the brass wire adheres to a machined surface under rough machining conditions in wire EDM. Since area A is a rough machined surface, much of the wire electrode components adhere to the machined surface. Since the formation of TCP is concentrated only in area A, it is considered that the reaction of the region including brass wire components and SBF affects TCP precipitation.

5. Conclusions

(1) A significant amount of TiO was ununiformly formed on the die-sinking EDMed surface of titanium generated using a copper electrode in deionized water.

(2) Although a uniform TiO_2 layer could be formed on the machined surface by wire EDM processing, the formation of hydroxyapatite was not confirmed after SBF immersion.

(3) The white material precipitated on the titanium wire-EDMed surface in SBF was low-crystallinity and formed in uniformly nucleation. The white precipitate was determined to be osteoconductive TCP by Raman spectroscopic analysis and by its precipitation mechanism. Therefore, osteoconductivity can be added to titanium surfaces by EDM in deionized water.

(4) When a brass electrode was used in wire EDM, the uniform formarion of TCP was enabled by the uniform distribution of brass components on the EDMed surface.

Acknowledgements

We would like to express special thanks to Mr. Mitsuomi Kimura of Teijin Nakashima Medical Co., Ltd., for his cooperation in the progress of this study.

References:

[1] T. Albrektsson, P.I. Bråemark, H.A. Hansson, B. Kasemo, K.Larsson, I. Lundström, D. H. McQueen, and R. Skalak., "The interface zone of inorganic implantsIn vivo: Titanium implants in bone," Ann. Biomed. Eng., Vol.11, pp. 1-27, 1983.

[2] X. Liua, P.K. Chub, and C. Ding, "Surface modification of titanium, titanium alloys, and related materials for biomedical applications," Materials Science and Engineering R,Vol.47, pp. 49-121, 2004.

[3] J. A. DiPisa, G. S. Sih, and A. T. Berman, "The Temperature Problem at the Bone-Acrylic Cement Interface of the Total Hip Replacement," Clin. Orthop, Res., Vol.121, pp. 95-98, 1976.

[4] W. Petty, "Methyl methacrylate concentrations in tissues adjacent to bone cement," J. Biomed. Mater. Res., Vol.14, pp. 427-434, 1980.
[5] H. Yoshikawa, T. Nakano, A. Matsuoka, and Y. Nakashima, "Miraigatajinkoukansetsuwomezashite – sonorekishikara shouraitenboumade –," NIHON IGAKUKAN, p. 299, 2013 (in Japanese).
[6] L. Sun, C. C. Berndt, K. A. Gross, and A. Kucuk, "Material fundamentals and clinical performance of plasma-sprayed hydroxyapatite coatings: A review," J. Biomed. Mater. Res., Vol.58, pp. 570-592, 2001.
[7] T. D. Driskell, "Early History of Calcium Ohosphate Materials and Coatings," Philadelphia: ASTM Publication, p. 3, 1994.
[8] W. R. Lacefield, "An Introduction to Bioceramics," L. L. Hench, J. Wilson (Eds.), Singapore: World Scientific, p. 223, 1993.
[9] K. de Groot, R. G. T. Geesink, C. P. A. T. Klein, and P. Serekian, "Plasma sprayed coatings of hydroxyapatite," J. Biomed. Mater. Res., Vol.21, pp. 1375-1381, 1987.
[10] L. H. Li, Y. M. Kong, H. W. Kim, Y. W. Kim, H. E. Kim, S. J. Heo, and J. Y. Koak, "Improved biological performance of Ti implants due to surface modification by micro-arc oxidation," Biomaterials, Vol.25, pp. 2867-2875, 2004.
[11] Y. Tsutsumi, M. Niinomi, M. Nakai, H. Tsutsumi, H. Doi, N. Nomura, and T. Hanawa, "Micro-arc oxidation treatment to improve the hard-tissue compatibility of Ti–29Nb–13Ta–4.6Zr alloy," Appl. Surf. Sci. Vol.262, pp. 34-38, 2012.
[12] J. Lu, M. P. Rao, N. C. MacDonald, D. Khang, and T. J. Webster, "UV-enhanced bioactivity and cell response of micro-arc oxidized titania coatings," Acta Biomater. Vol.4, pp. 1518-1529, 2008.
[13] A. Sugino, K. Uetsuki, K. Tsuru, S. Hayakawa, A, Osaka and C. Ohtsuki, "Surface Topography Designed to Provide Osteoconductivity to Titanium after Thermal Oxidation," Materials Trans., Vol.49, No.3, pp. 428-434, 2008.
[14] M. Mizutani, R. Honda, Y. Kurashina, J. Komotori, and H. Ohmori, "Improved Cytocompatibility of Nanosecond-Pulsed Laser-Treated Commercially Pure Ti Surfaces," Int. J. of Automation Technology, Vol.8, No.1, pp. 102-109, 2014.
[15] M. Mizutani, N. Masuko, R. Honda, R. Murakami, J. Komotori, and T. Kuriyagawa, "Creation of bioactive surfaces by nanosecond-pulsed laser irradiation of commercially pure titanium," J. of the Japan Society for Abrasive Technology, Vol.59, No.1, pp. 17-22, 2015.
[16] H. Takezawa, N. Mohri, K. Asano, and Y. Kodama, "Development of Micro Electrical Discharge Machine," Int. J. of Automation Technology, Vol.2, No.2, pp. 124-130, 2008.
[17] K. Furutani, "Proposal for Abrasive Layer Fabrication on Thin Wire by Electrical Discharge Machining," Int. J. of Automation Technology, Vol.8, No.1, pp. 394-398, 2014.
[18] T. Kokubo, and T. Takadama, "How useful is SBF in predicting in vivo bone bioactivity? Biomaterials," Vol.27, pp. 2907-2915, 2006.
[19] T. Kokubo, H. Kushitani, S. Sakka, T. Kitsugi, and T. Yamamuro, "Solution able to reproduce in vivo surface – structure changes in bioactive glass-ceramic A-W," J. Biomed. Mater. Res, Vol.24, pp. 721-734, 1990.
[20] ISO 23317:2007, "Implants for surgery. In vitro evaluation for apatite-forming ability of implant materials."
[21] S. V. Dorozhkin, "Medical application of calcium orthophosphate bioceramics," BIO, Vol.1, pp. 1-51, 2011.

Name:
Togo Shinonaga

Affiliation:
Graduate School of Natural Science and Technology, Okayama University

Address:
3-1-1 Tsushima-naka, Kita-ku, Okayama 700-8530, Japan

Brief Biographical History:
2013- Research Fellow of Japan Society for the Promotion of Science, Joining and Welding Research Institute, Osaka University
2015- Assistant Professor, Okayama University

Main Works:
• "Formation of periodic nanostructures using a femtosecond laser to control cell spreading on titanium," Applied Physics B: Lasers and Optics, Vol.119, pp. 493-496, 2015.
• "Prediction of rounding phenomenon at corner tips in large-area Electron Beam irradiation," Int. J. of Machine Tools and Manufacture, Vol.110, pp. 18-26, 2016.

Membership in Academic Societies:
• Japan Society of Precision Engineering (JSPE)
• Japan Laser Processing Society (JLPS)
• Japan Society of Mechanical Engineering (JSME)
• Laser Society of Japan (JLS)
• Japan Society of Applied Physics (JSAP)
• Institute of Electrical Engineers of Japan (IEEJ)

Name:
Yuta Iida

Affiliation:
Student, Graduate School of Natural Science and Technology, Okayama University

Address:
3-1-1 Tsushima-naka, Kita-ku, Okayama 700-8530, Japan

Brief Biographical History:
2017- Master's Course Student, Graduate School of Natural Science and Technology, Okayama University

Membership in Academic Societies:
• Japan Society for Precision Engineering (JSPE)

Name:
Ryota Toshimitsu

Affiliation:
Student, Graduate School of Natural Science and Technology, Okayama University

Address:
3-1-1 Tsushima-naka, Kita-ku, Okayama 700-8530, Japan

Brief Biographical History:
2015- Master's Course Student, Graduate School of Natural Science and Technology, Okayama University

Membership in Academic Societies:
• Japan Society of Mechanical Engineers (JSME)

Name:
Akira Okada

Affiliation:
Professor, Graduate School of Natural Science and Technology, Okayama University

Address:
3-1-1 Tsushima-naka, Kita-ku, Okayama 700-8530, Japan

Brief Biographical History:
2004- Associate Professor, Okayama University
2011- Professor, Okayama University

Main Works:
• "Improvement of Surface Characteritics for Long Life of Metal Molds by Large-area EB Irradiation," J. of Material Processing Technology, Vol.214, No.8, pp. 1740-1748, 2014.
• "Computational Fluid Dynamics Analysis of Working Fluid Flow and Debris," CIRP Annals Manufacturing Technology, Vol.58, No.1, pp. 209-212, 2009.
• "A New Slicing Method of Monocrystalline Silicon Ingot by Wire EDM," Int. J. of Electrical Machining, No.8, pp. 21-26, 2003.

Membership in Academic Societies:
• International Academy for Production Engineering (CIRP)
• Japan Society of Mechanical Engineers (JSME)
• Japan Society for Precision Engineering (JSPE)
• Japan Society of Electrical Machining Engineers (JSEME)
• American Society for Precision Engineering (ASPE)
• Japan Society for Die and Mould Technology (JSDMT)